

Collision induced desorption of N₂ from Ru(001)

L. Romm

*Department of Physical Chemistry and the Farkas Center for Light Induced Processes,
The Hebrew University, Jerusalem, 91904, Israel*

Y. Zeiri

Department of Chemistry, Nuclear Research Center, Negev, P.O.B. 9001, Beer-Sheva, Israel

M. Asscher

*Department of Physical Chemistry and the Farkas Center for Light Induced Processes,
The Hebrew University, Jerusalem 91904, Israel*

(Received 11 August 1997; accepted 17 February 1998)

The dynamics of collision-induced desorption (CID) of N₂ from Ru(001) exposed to hyperthermal rare gas colliders generated in a supersonic atomic beam source have been studied. Low coverage of 0.01 ML ¹⁵N₂ at crystal temperature of 96 K was chosen to represent a CID process of a practically isolated molecule, neglecting the effect of lateral N₂-N₂ interactions. The cross sections for CID of nitrogen molecules, $\sigma_{\text{des}}(E_i, \theta_i)$, as a function of the kinetic energy and angle of incidence of Ar and Kr colliders have been measured. It was found that $\sigma_{\text{des}}(E_i, \theta_i=0^\circ)$ changes monotonically in the range 0–25 Å² for beam energy in the range of 0.5–5.5 eV and is insensitive to the type of collider (Ar, Kr) as well as to the adsorbate isotope (¹⁴N₂, ¹⁵N₂). The threshold energy for desorption has been determined to be 0.50±0.10 eV, which is twice the binding energy of N₂ to Ru(001). The cross section for CID at a fixed collider's energy rises approximately four times as the incidence angle θ_i increases from 0° to 70° relative to the surface normal. Neither normal nor total energy scaling of the cross section could describe the results. The $\sigma_{\text{des}}(\theta_i)$ scales reasonably well, however, with the tangential energy of the collider for angles above 30°. Classical molecular dynamics simulations were performed to gain better understanding of the CID process. Threshold energy and angular dependence of the cross section were reproduced very well. The predominant CID mechanism was concluded to originate from a direct rare gas–nitrogen collision, in which impulsive-bending and the motion along the surface are coupled to the adsorbate motion which leads to desorption. © 1998 American Institute of Physics. [S0021-9606(98)01020-4]

I. INTRODUCTION

Among the elementary steps of heterogeneous catalysis, thermal desorption is probably the best studied and most frequently used to characterize the adsorbed gas.¹ Under industrial high pressure conditions, in addition to thermal desorption one should consider the effect of energetic colliders from the gas phase on the adsorbates. It was suggested theoretically by Zeiri and co-workers² and then shown experimentally by Ceyer and co-workers,^{3–5} that energetic colliders can indeed induce desorption of adsorbates. It was argued that such energetic colliders should exist in the tail of the Boltzmann distribution at high pressures, therefore collision induced desorption (CID) should be considered and taken into account while simulating kinetic processes at the industrial conditions.

Details of the dynamics of the CID process can provide important information about the interaction potential between the adsorbate and the solid surface. The link between experimental data and the interaction potentials in the system investigated is provided by molecular dynamics simulations. The classical calculations are justified since in the energy range relevant to CID quantum effects (i.e., tunneling and nonadiabatic transitions) can be ignored.

In their first experimental CID study, Ceyer and

co-workers^{3–5} have investigated the dynamics of CH₄ desorption from Ni(111), induced by energetic Ar beam. They have determined the dependence of the cross section for desorption on the initial Ar kinetic energy and angle of incidence. Results of classical trajectory calculations treating methane and argon as hard spheres and the surface as a rigid wall (hard cube^{8,9}) have reproduced the experimental trends very well indicating that the dominant mechanism for CID is a direct impulsive collision of the incident Ar atom with the physisorbed CH₄. The same hard cube model has been later employed by Levis and co-workers^{10–12} to obtain the binding energy of an adsorbate (NH₃ and C₂H₄ in their study) to a metal surface [Pt(111) in the above study] from the threshold energy necessary to induce CID. Classical molecular dynamics (MD) simulations of the CID process by Zeiri and co-workers^{2,13–15} have indicated the importance of direct impact in their study of the CID of Xe from Si by impinging Xe atoms,² N₂ from W(100) by Ar atoms¹³ and Ar from W(100) by Xe atoms.¹⁴ For glancing angles of incidence, however, an additional pathway for desorption occurs via indirect mirrorlike collisions of the gas atom with the surface prior to collision with the adsorbate.¹³ A very recent study by Rettner and co-workers,¹⁶ has combined experimental study with MD simulations of the CID of Xe from Pt(111) induced

by energetic Ar colliders. The results of both hard-cube and full MD approaches were in good agreement with the experimental data in the case of the isolated adsorbate (low coverage). They show that CID occurs via either direct gas/adsorbate–adsorbate/surface collision or indirect gas/surface–gas/adsorbate collisions.

In this work, we present the results of an experimental study in which the CID of N_2 from Ru(001) using Ar and Kr supersonic atomic beams has been investigated. The nitrogen molecule is known to weakly chemisorb on Ru(001) with its molecular axis perpendicular to the surface plane,^{17–19} similar to the isoelectronic CO molecule, but at far lower binding energy to the surface.¹⁷ The results are limited to low coverages in the range of a few percent of a monolayer of nitrogen. The dynamics of the CID have been studied by measuring the absolute cross section for desorption as a function of incidence angle and energy of the collider. MD simulations of the Ar/ N_2 /Ru(001) system²⁰ have been performed parallel to the experimental work, but only a brief description of the results of these simulations will be presented here. Full account of the theoretical study will be given elsewhere.²⁰

Our choice of the N_2 /Ru system has been motivated by its relevance to the ammonia synthesis, where molecular nitrogen dissociation proceeds via a large activation barrier,²¹ therefore it is the rate limiting step. Ruthenium is known as the best “noniron” catalyst.⁶

II. EXPERIMENT

The experiments reported here were conducted in an atomic beam–surface scattering chamber equipped with standard surface cleaning and characterization tools. The base pressure was 1×10^{-10} Torr, rising to 2×10^{-8} Torr when the beam is on. The supersonic beam of seeded Ar or Kr in He has been generated in a differentially pumped section composed of three chambers, separated by a single skimmer and two collimating apertures. Typical pressures in the source (1200 ℓ /s diffusion pump), first (700 ℓ /s diffusion pump) and second (50 ℓ /s turbopump) differentially pumped chambers, when the beam is on were 5×10^{-4} Torr, 1×10^{-5} Torr, and 5×10^{-7} Torr, respectively. A laser drilled stainless steel nozzle with an orifice of about 70 μ m, water cooled, could be resistively heated to 1400 K. The apertures at the first and second differentially pumped chambers were made such that the beam diameter is slightly larger than the sample at the center of the UHV scattering chamber, ensuring homogeneous distribution of the rare gas atoms striking the sample. Nozzle to sample distance is 90 cm. A 400 Hz chopper (50 mm diameter, 0.5 mm thickness, single 0.5 mm) slit stainless-steel disk on a compact synchronous gyromotor (Condor Pacific Ltd.), in the first differentially pumped chamber has been employed to determine the velocity distributions of the incident rare gas atoms. These distributions were determined at a distance of 49.8 cm from the chopper in the open ionizer of a quadrupole mass spectrometer positioned perpendicular to the beam axis, inside the UHV chamber. The current signal was extracted directly from the channeltron and amplified before it was analyzed by a TDS-520 digitizing oscilloscope. Instrumental velocity resolution is estimated at $\Delta V/V \approx 0.2$.

The most probable velocity was used to define the incident kinetic energy and from the width of the velocity distribution an energy spread— $\Delta E/E \approx 0.4$ was deduced for nozzle at room temperature. At nozzle temperature of 1400 K, the distribution increases to $\Delta E/E \approx 0.5$. Sample preparation of the Ru(001) crystal has followed standard procedures, which include Ar⁺ ion sputter at 600 V followed by oxygen treatment (5×10^{-8} Torr oxygen over sample at 1070 K for 5 minutes) and then annealing at 1600 K for 3 min resulted in very steep LEED spots with the proper hexagonal symmetry. Cleanliness was determined by Auger spectroscopy using hemispherical electron energy analyzer (Clam-100, VG). The surface temperature determination has been obtained using W26%Re–W5%Re thermocouple spot-welded to the back side of the sample. This enabled computer controlled ac-resistive heating procedure to generate linear heating rates or stabilized temperatures at accuracy of ± 0.5 K.

Adsorbed $^{15}N_2$ at a coverage of 0.03 of the saturation value (calibrated by TPD) at crystal temperature of 96 K has been obtained by backfilling the UHV chamber. This coverage is equivalent to a ratio of N_2 /Ru=0.01.²² Detection of collision induced desorption rates has been performed by monitoring the quadrupole signal at $e/m=30$ as a function of time before and during the exposure to the atomic beam. At this low coverage regime, exponential decays of the CID signal which terminates at zero, were obtained only if the pumping around the quadrupole has been improved, namely after removing the glass cover over the quadrupole, a scheme usually used for TPD measurements.

III. RESULTS

Evaluation of the influence of various dynamical parameters such as angle of incidence and energy of the collider on the yield of collision induced desorption requires a definition of the cross section for CID. The cross section for CID is thus defined^{23,5} as an area on the surface in which an impact of rare gas atom yields a single CID event per one adsorbed nitrogen molecule. In the limit of very low N_2 initial coverage CID is governed by first order reaction kinetics since the interaction between neighbor nitrogen molecules can be neglected. The only initial coverage employed in the present study is $\Theta=0.01$ ML (1 nitrogen molecule per 100 Ru atoms), hence the average distance between two neighbor N_2 molecules is ~ 27 Å. Therefore, a first order rate equation⁵ is used to describe the CID kinetics

$$-\frac{\partial \Theta(t)}{\partial t} = \sigma_{\text{des}}(E_i, \vartheta_i) \cdot F \cdot \Theta(t), \quad (1)$$

where $\Theta(t)$ is the time dependent coverage of nitrogen, F is the flux of the incident rare gas atom beam, σ_{des} is the absolute cross section for CID, E_i , ϑ_i are the initial energy and angle of incidence of the collider, respectively. The beam flux is defined as the number of rare gas atoms impacting the surface per unit area per unit time, $F = F_{\text{abs}} \cdot \cos \theta_i$, F_{abs} is the absolute flux measured normal to the beam axis.

At the crystal temperature of 96 K used during the CID experiments, none of the beam atoms (He, Ar, or Kr) stick to the surface, therefore the adsorbed nitrogen molecule can be

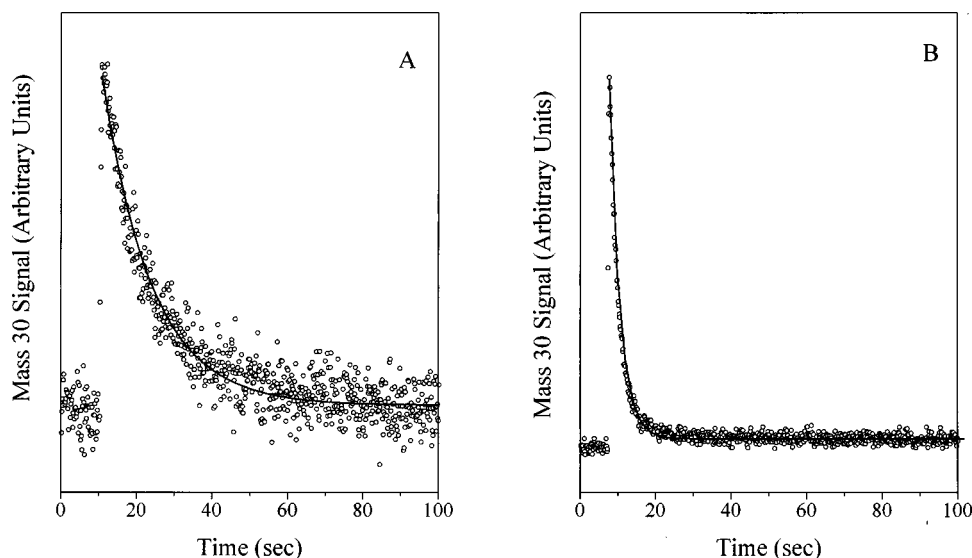


FIG. 1. N_2 (mass 30) pressure change as a result of collision induced desorption (CID) by Ar/Kr atoms from a supersonic beam. (A) E_i (Ar)=0.9 eV, $\theta_i = 0^\circ$, (B) E_i (Kr)=3.3 eV, $\theta_i = 0^\circ$. The Ru(001) surface is preadsorbed with 0.01 ML of $^{15}N_2$ at $T_s = 96$ K. The points show experimental data, and the lines present a first order exponential decay fit. A sharp rise in pressure indicates that a beam shutter has been opened and the sample has been exposed to the atomic beam.

considered isolated. It was experimentally verified that pure He beam does not induce any desorption of nitrogen up to the highest nozzle temperature of 1400 K. In principle, dissociation of the adsorbed nitrogen molecule may occur as a result of collision with energetic rare gas atom from the beam, as was shown for the case of CH_4 on Ni(111).²⁴ However, the probability for such collision-induced dissociation must be extremely small and is definitely below the detection limit of our TPD. This conclusion is based on experiments with very high kinetic energy of the colliders of up to ~ 8 eV (checked with Xe seeded in He) which resulted in absolutely no dissociation. Therefore, collision-induced dissociation is not considered in this paper.

It was experimentally verified that the CID signal is not sensitive to the position of the sample with respect to the beam when the measurements were performed at nonzero angles of incidence, indicating the uniformity of the colliders flux at the sample position. Readsorption of the CID molecules was also negligible.

In the low coverage limit, σ_{des} does not depend on $\Theta(t)$, therefore, integrating Eq. (1) we obtain

$$\Theta(t) = \Theta_0 \cdot e^{-\sigma_{des} \cdot F \cdot t}. \quad (2)$$

The instantaneous nitrogen partial pressure $P(t)$ in the UHV chamber is proportional to the nitrogen coverage $\Theta(t)$ on the Ru(001) surface, $P(t) \propto \Theta(t)$. Thus knowing the absolute beam flux, we can extract the magnitude of the CID cross section from the first-order exponential decay of the nitrogen partial pressure as a function of time after exposing the adsorbed nitrogen to the atomic beam. This procedure is thus repeated for various kinetic energies and angles of incidence of the collider, in order to obtain the full dynamical response of σ_{des} . The absolute atomic beam flux is determined from the partial pressure rise produced by the beam in the UHV chamber by the following expression:²⁵

$$F_i = \frac{\Delta P_i \cdot \eta \cdot N}{S_{beam}}, \quad (3)$$

where F_i (atoms \times cm⁻² \times s⁻¹) is the absolute flux, ΔP_i (Torr) is the pressure rise when the beam is on, η (cm³/s) is the system pumping speed (typically 5×10^5 cm³/s), N is the number of atoms in cm³ at 1 Torr and S_{beam} (cm²) is the effective beam area at the sample.

Two examples of the changing nitrogen partial pressure as a function of time $P(t)$ when the beam is on and their exponential best fit are shown in Fig. 1. First-order exponential decays fit very well the experimental data, therefore the CID cross section can be directly derived from the fit. The cross sections presented below are the result of averaging of the fit parameters for two to three of these pressure measurements at identical conditions of the beam.

In Fig. 2 the dependence of the cross section for CID on the kinetic energy of the collider (both Ar and Kr) for a fixed angle of incidence, normal to the surface, is shown. As expected, σ_{des} increases with the kinetic energy of the collider atom. Saturation of the cross section is not observed even at the highest kinetic energies of 5.5 eV. The σ_{des} is insensitive to the mass of the collider. We have also checked the role of mass of the adsorbate, having $^{14}N_2$ vs $^{15}N_2$ on the surface and found no effect of the mass of the adsorbed nitrogen on the σ_{des} .

The effect of angle of incidence, θ_i , of the collider on the CID cross section has been investigated by varying the angle in the range 0–70 deg measured relative to the surface normal. The cross section was found to be rather sensitive to θ_i , as seen in Fig. 3. The magnitude of σ_{des} rises approximately four times as θ_i increases from 0° to 70°.

The threshold energy for collision-induced desorption was not directly measured due to experimental uncertainties below cross sections of 2 Å². We have determined the

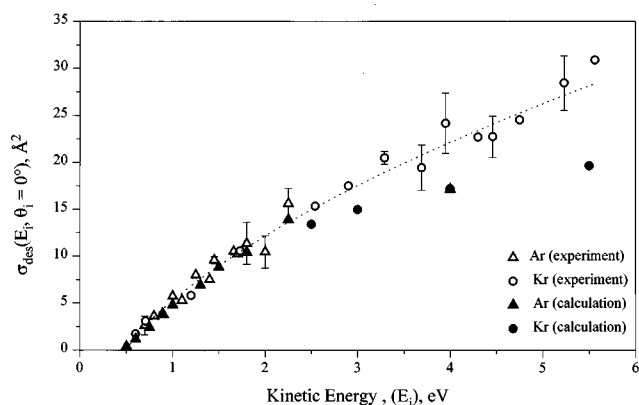


FIG. 2. Cross section for CID of 0.01 ML $^{15}\text{N}_2$ as a function of kinetic energy of the collider at normal incidence. Triangles represent Ar, circles—Kr. The results of full classical MD calculations (see the text below) are shown for comparison. Dotted curve is a guide to the eye.

threshold by extrapolation of the $\sigma_{\text{des}}(E_i)$ curve to zero using the empirical expression below. This equation has been frequently used in gas phase studies where empirical threshold energy for reactivity could be determined^{11,26}

$$\sigma_{\text{des}} = \frac{A}{E_i} (E_i - E_{\text{thr}})^n, \quad (4)$$

where E_i is the total incident kinetic energy of the collider, E_{thr} is a threshold energy, A and n are fitting parameters. The parameter A has the physical meaning of an effective geometrical cross section for CID. The geometrical cross section, given by $\pi(r_{\text{ads}} + r_{\text{gas}})^2 / \cos \theta_i$ (r_{ads} and r_{gas} are the adsorbate and the rare gas collider radii, respectively), is defined as the net area on the surface per adsorbate, inside of which an incident particle cannot strike without colliding with an adsorbate.^{5,16} The changing value of A is displayed in the inset of Fig. 4, where $n = 1.3 \pm 0.2$. Nonlinear least squares fitting curves are presented in Fig. 4 for three different angles of incidence (dotted lines). The threshold energy for CID [calculated using Eq. (4)] is found to be practically independent of the angle of incidence.

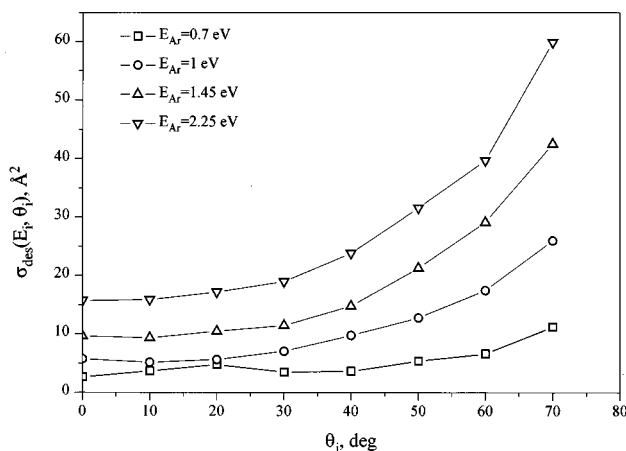


FIG. 3. Angular dependence of the CID cross section at the indicated kinetic energies of the Ar collider.

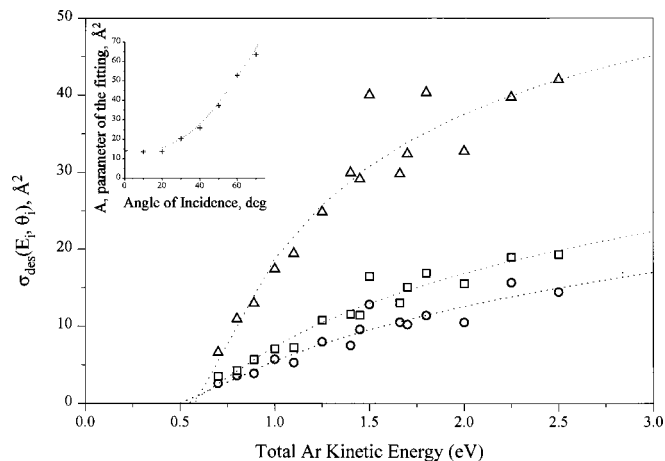


FIG. 4. Cross section for CID plotted vs the total kinetic energy of the collider at the following angles of incidence: circles — $\theta_i = 0^\circ$, squares — $\theta_i = 30^\circ$, triangles — $\theta_i = 60^\circ$. The dotted lines present the results of the best nonlinear least squares fit based on Eq. (4).

A reactive CID event requires that the adsorbate motion in the direction normal to the surface should gain sufficient kinetic energy, in order to overcome the binding energy to the surface. It is instructive, therefore, to isolate the role of the normal energy component of the collider on the final experimentally determined CID cross section. In Fig. 5 we have plotted the experimentally determined CID cross sections σ_{des} vs the normal energy component for various angles of incidence and kinetic energies. The data points which pertain to a given angle of incidence, were found to follow Eq. (4) above, when the normal energy E_\perp replaces the total energy E_i for each of these data points. The same parameter $n = 1.3 \pm 0.2$, as in Fig. 4, and very similar behavior of A are obtained from the best fits throughout the entire set of data points (inset of Fig. 5).

The threshold normal energies obtained by the extrapolation to zero of the data points in this normal energy pre-

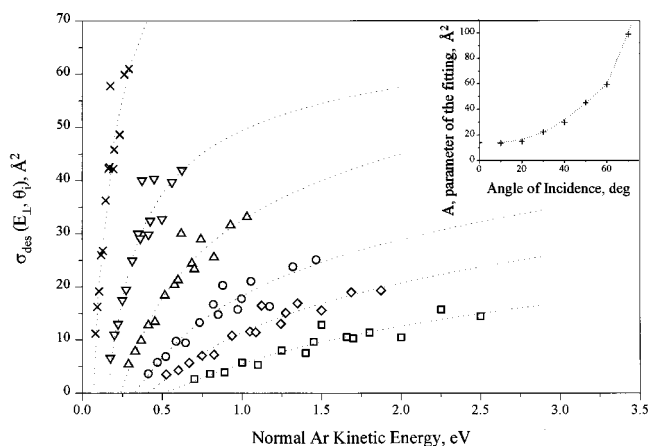


FIG. 5. Cross section for CID plotted vs the normal kinetic energy component ($E_\perp = E_i \cos^2 \theta_i$) of the collider at the following angles of incidence: squares — $\theta_i = 0^\circ$, diamonds — $\theta_i = 30^\circ$, circles — $\theta_i = 40^\circ$, up triangles — $\theta_i = 50^\circ$, down triangles — $\theta_i = 60^\circ$, crosses — $\theta_i = 70^\circ$. As in Fig. 4, dotted lines show the best fit based on Eq. (4) (see the text).

sensation, are found to *decrease* from 0.5 eV at normal incidence to less than 0.1 eV at incidence angle of 70° .

The CID cross section is found to be particularly sensitive to the parallel energy component ($E_{\parallel} = E_i \sin^2 \theta_i$), as evidenced by the fast increase of σ_{des} with energy at the large incidence angles. For example, at θ_i at 70° , the CID cross section increases by a factor of 6, while the normal energy increases only by a factor of 2.5, from 0.1 to 0.25 eV.

IV. DISCUSSION

A. Normal incidence

In Fig. 2 the cross section for CID as a function of kinetic energy of the collider atom for normal angle of incidence is presented. The cross section increases monotonically with the collider kinetic energy up to the maximum energy of 5.5 eV employed in the present study. Essentially, the CID event consists of few elementary steps.⁵ A rare gas atom collides with the adsorbed N_2 transferring part of its kinetic energy. As a result, the adsorbate moves towards the surface and stops at the turning point. If the kinetic energy transferred from the rare gas atom is equal or greater than the threshold energy for desorption, the adsorbate will have sufficient energy to escape the attractive part of the PES to the gas phase provided that its loss of energy to the solid is negligible. As the initial kinetic energy of the collider increases, more energy is transferred to the adsorbate. Hence, the minimum energy transfer required for completion of CID can occur at larger impact parameters which correspond to an increase of σ_{des} . The energy transferred to the adsorbate, induces excitation of internal degrees of freedom of the adsorbate, mostly rotation.

From previous CID studies of $\text{NH}_3/\text{Pt}(111)$ ¹¹ and $\text{CH}_4/\text{Ni}(111)$ ⁵ as in our case, the mechanism of the CID event is basically an impulsive direct collision between the incoming rare gas atom and the adsorbate. However, desorption which proceeds via this mechanism should show a saturationlike behavior of the cross section at higher kinetic energies. This arises from the fact that the geometrical cross section for the interaction between the collider and the adsorbate, defined as $\pi(r_{\text{ads}} + r_{\text{gas}})^2 / \cos \theta_i$,^{5,16} where r_{ads} and r_{gas} are the hard sphere radii of the adsorbate and rare gas collider, respectively, reaches its maximum value when their separation distance equals the sum of their hard sphere (van der Waals) radii. In the case of N_2 and Kr as the collider, the sum of the hard sphere radii is $\sim 3.5 \text{ \AA}$, hence a maximum geometrical cross section for normal incidence is expected at $\sim 38 \text{ \AA}^2$. Extrapolating the $\sigma_{\text{des}}(E_i, \theta_i = 0^\circ)$ curve (Fig. 2) to the maximum possible cross section, we find that an initial kinetic energy of about 14 eV is required to observe the saturation value of σ_{des} . This magnitude of collider's kinetic energy was not available in our experiments, therefore saturation could not be reached.

Another mechanism for CID—"hot spot" formation upon collision of the energetic gas atom with the surface at large impact parameters needs also to be considered. This mechanism, however, cannot be important since the energy dissipation from the hot spot has a time scale comparable to the period of N_2 -Ru single vibration.^{13,28} This time is appar-

ently insufficient to cause the necessary energy flow to the molecule-metal bond. Consequently, the thermally activated desorption initiated by a distant hot-spot should be ruled out.

B. Threshold energy for CID and angular dependence of σ_{des}

The threshold energy (E_{thr}) for CID is defined as the minimum energy of the collider needed to induce the desorption of an adsorbate from the surface. In the first detailed experimental study of the CID of CH_4 from $\text{Ni}(111)$ by argon, studied by Beckerle, Johnson, and Ceyer (BJC), the threshold at normal incidence has been determined to be three times the binding energy of methane to nickel.⁵ In the recent study of CID of Xe from $\text{Pt}(111)$ by argon, Kulginov, Persson, and Rettner (KPR) have reported the threshold to be almost four times the binding of xenon to $\text{Pt}(111)$.¹⁶ Levis and co-workers¹⁰⁻¹² have measured the threshold energy for CID of NH_3 from $\text{Pt}(111)$ and $\pi\text{-C}_2\text{H}_4$ from $\text{O}/\text{Pt}(111)$ at normal collider incidence. These authors have used the threshold energy to go back and evaluate the binding energy of these molecular adsorbates to the metal surface. They fitted calculated values to their data based on the hard sphere-hard cube (HSHC) model.^{5,8,9} This simple model treats the gas-metal and adsorbate-metal interactions as HSHC and the gas-adsorbate interaction as HSHS. They suggested an expression for the correlation between the binding energy of an adsorbate to the surface and the threshold kinetic energy at normal incidence of the rare gas atom collider.¹¹ KPR¹⁶ have extended the expression to include angular dependence and it looks as follows:

$$E_{\text{binding}} = E_{\text{threshold}} \frac{4m_{\text{col}}m_{\text{ads}}}{(m_{\text{col}} + m_{\text{ads}})^2} \times \left[1 - \frac{4m_{\text{ads}}m_M}{(m_{\text{ads}} + m_M)^2} \right] \cos^4(\theta_i/2). \quad (5)$$

In this model m_{col} and m_{ads} are the masses of the collider and adsorbate, respectively, while m_M is an effective mass of the metal substrate, equal to a few times the mass of the metal surface atom. Often, m_M is set at 3/2 times the real mass of the metal atom, indicating that the adsorbate interacts with more than a single substrate atom.²⁷ If we assume for a moment that the HSHC model applies to the $\text{N}_2/\text{Ru}(001)$ system, setting $m_M = 3/2 m_{\text{Ru}}$ and using our measured threshold energy of $0.5 \pm 0.1 \text{ eV}$ for the CID of N_2 by Ar at *normal incidence*, we obtain a binding energy of N_2 to $\text{Ru}(001)$ of 0.28 eV. This value is rather close to our independent measurements of the activation energy for desorption of N_2 from $\text{Ru}(001)$ of 0.25 eV obtained from lineshape analysis of TPD spectra with a pre-exponent factor $\nu_{\text{des}} = 1 \times 10^{12} \text{ s}^{-1}$.²⁸ The good agreement between the binding energy obtained from the simple HSHC model and the experimental data, suggests that this model indeed qualitatively captures the main contributing elements which dictate the threshold for the CID process, when limited to the normal incidence. It should be pointed out, however, that this model ignores the details of the interaction potentials between the adsorbate and the substrate, the collider-adsorbate and the collider-substrate. In

addition, the internal states of the adsorbate, which are shown to be excited by our MD simulations, are also ignored. This requires careful examination of all the available data before the HSHC model is adopted to describe the entire experimental CID results.

Using the HSHC model, one expects the threshold energy to rise as the angle of incidence of the collider, θ_i increases, a direct consequence of the normal energy scaling predicted by this model, as derived from Eq. (5). Our data, however, indicate that the threshold energy is practically insensitive to the angle of incidence. This is seen when the total energy presentation is used, namely the CID cross section vs total incidence energy of the collider is plotted for different angles of incidence, as shown in Fig. 4. As has been discussed in detail by BJC, at the same time that the normal energy component of the incident collider decreases with the increasing θ_i , the impact parameter range which leads to reactive CID event also increases.⁵ These opposing trends seem to be of the same magnitude in the case of the CID mechanism of N_2 from Ru(001). One may conclude, therefore, that this is the origin for the "total energy" scaling revealed in Fig. 4. This conclusion, however, is based on the assumption that the parallel momentum of the collider is conserved, as dictated by the HSHC model. This assumption is shown to be incorrect by the MD simulations described below.

When low energy particles strike a lighter adsorbate, multiple collisions of the adsorbate with the collider could significantly quench the kinetic energy of the adsorbate in the direction normal to the surface which may lead to desorption. The role of these multiple collisions on the threshold energy for CID at different angles of incidence has been extensively studied by BJC.⁵ Their conclusions were derived from MD simulations based on HSHC model. Multiple collisions were found to be important factor at small angles of incidence near the threshold energy (observed at small impact parameters), causing the threshold energy to rise close to normal incidence when compared to larger angles of incidence. The combination of the effects of diminishing normal energy component and the increasing number of reactive trajectories at larger impact parameters at the large angles of incidence on one hand, but at the same time the influence of multiple collisions at close to normal incidence, were used to explain the deviation from "simple" normal energy scaling in CID.⁵ In the CID mechanism of our system, however, multiple collisions were found to be unimportant, as shown by the MD simulations discussed below in Sec. IV C.

Careful examination of Fig. 4 reveals that the threshold energy for CID is not precisely incident angle independent. This may arise from uncertainty in the experimental data but it may also originate from deeper mechanistic reasons. In order to clarify this point, we have isolated the net contribution of the normal momentum transfer (normal energy component) to the CID process. This is done by plotting the CID cross sections σ_{des} vs the collider's normal kinetic energy E_{\perp} for different angles of incidence, as demonstrated in Fig. 5. A fit to the data points is obtained using Eq. (4), after replacing the total energy E_i by E_{\perp} .

Normal energy scaling in CID, may be reflected in the

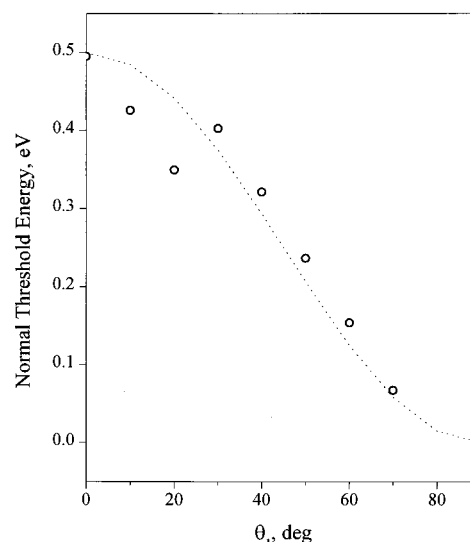


FIG. 6. Threshold of normal energy component plotted vs angle of incidence of the collider. (Total energy is $E_i = 0.5$ eV of Ar as a collider.) The dotted line corresponds to the expression $E_{\perp, \text{thr}} = 0.5 \cdot \cos^2 \theta_i$.

threshold energy for this process, if the normal momentum is the only component to be transferred to the adsorbate and directly contribute to the CID process. The parallel momentum should be conserved in such a case and cannot be converted into molecular motion in the direction normal to the surface. A plot of the CID cross section vs the normal energy for various angles of incidence, should result in a fixed threshold energy. The experimental data indicate, however, that the threshold energy decreases as θ_i increases, as shown in Fig. 5. In fact, the threshold energy obtained from this plot decreases as $\cos^2 \theta_i$, as seen in Fig. 6.

All these pieces of information strongly indicate that in our system the parallel momentum transfer is of great importance for the CID mechanism. The momentum transfer from the collider to the adsorbed nitrogen molecule along the surface plane may only be effective for CID if there is a strong coupling between the motion of the adsorbate parallel to the surface and normal to it. Such coupling may arise from a significant corrugation in the N_2 -Ru interaction potential energy surface. In addition, polarization and anisotropy in the bonding of the nitrogen molecule to the surface, which leads to adsorption geometry with the molecular axis normal to the surface, result in a strong coupling between the impulsive-tilt-motion (ITM) of the adsorbate during the energetic collision and its motion in the direction away from the surface. It is important to note that internal states excitation (mostly rotation) somewhat increase the threshold energy, when compared with the CID process of atoms.¹⁶ This effect must be taken into account in a realistic MD simulation, as is discussed below.

The enhancement of the cross section for CID with increasing angle of incidence (see Fig. 3) provides new insight into the mechanism of the CID event. The interplay between the normal energy component and the geometrical cross section as θ_i increases and their opposing effects have been discussed by BJC.⁵ The increase of σ_{des} with the angle of incidence is almost twice faster, however, in the case of

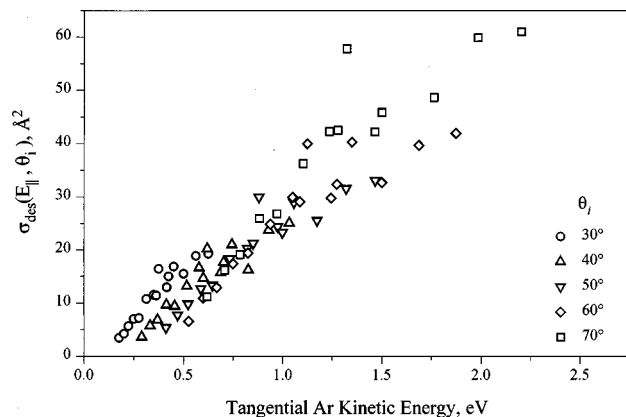


FIG. 7. Cross section for CID plotted vs the tangential kinetic energy component ($E_{\parallel}=E_i \cdot \sin^2 \theta_i$) of the collider at different angles of incidence.

$\text{N}_2/\text{Ru}(001)$ compared with the $\text{CH}_4/\text{Ni}(111)$ system.⁵

The rapid increase of σ_{des} as θ_i increases implies that a new mechanism for CID becomes dominant as the angle of incidence increases. Transfer of momentum parallel to the surface ($P_{\parallel}=P_i \cdot \sin \theta_i$) induces the adsorbate motion along the surface plane. It can also induce a significant impulsiv-tilt-motion (ITM) which “shakes-up” the on-top N_2 adsorption geometry with its molecular axis normal to the surface.^{17–19,22,29} The role of the tangential energy transfer may, therefore, be explained by a corrugated $\text{N}_2\text{--Ru}(001)$ PES which leads to the efficient coupling between tilt and parallel motions and the motion normal to the surface.

We conclude that within the experimental uncertainties of our work the CID of N_2 from $\text{Ru}(001)$ approximately scales with the tangential energy of the collider (Fig. 7). Similar conclusions regarding the importance of the parallel momentum transfer for CID processes has very recently been indicated in the $\text{O}_2/\text{Ag}(100)$ system.³⁰

While the above mentioned mechanism for the conversion of parallel to normal motion implies that direct collision between the gas atom and the adsorbate is dominant, an additional mechanism for the CID event should be considered. This mechanism is expected to be particularly relevant at close to glancing angles of incidence and has been discussed by Zeiri¹³ and BJC.⁵ It involves indirect mirror collisions, where the gas atom which scatters first from the surface collides with the adsorbate on its way back to the gas phase. In principle, mirror collisions which result in CID, are likely to occur at very large impact parameters.

In the present study, this type of CID mechanism is not important, as concluded from the MD simulations described below. This is primarily due to details of the PES of the collider rare gas atoms with the surface.²⁰

C. Molecular dynamics simulations

In order to better understand the details of the CID dynamics of N_2 from $\text{Ru}(001)$ we have performed stochastic classical molecular dynamics (MD) simulations. Employing MD simulations, we also try to resolve the difficulties which arise from the interpretation of the experimental data on the basis of the simple HSHC model discussed above. Only a

brief description of the results obtained from the MD simulations which directly pertain to the experimental results discussed above is given here, more details will be presented elsewhere.²⁰

A semiempirical potential energy surface representing the rare gas/ $\text{N}_2/\text{Ru}(001)$ interactions has been constructed.²⁰ The solid is described by a slab of two moveable metal atom layers, composed of 56 atoms in each layer, positioned on top of two additional layers, which were kept fixed at their lattice points. Periodic boundary conditions along the directions parallel to the surface plane were used. The motion of the metal atoms is assumed to be harmonic.³¹ The infinite crystal is represented by coupling the bottom (movable) metal atom layer to a layer of fictitious particles whose time evolution is described by Langevine equations of motion. The $\text{N}_2\text{--Ru}$ interaction potential is similar to that described in Ref. 32, based on a sum of pairwise Morse potentials multiplied by an angular term to maintain normal adsorption geometry. The Ar--N_2 interaction is taken as a sum of pairwise Lennard-Jones potentials.¹³ Finally, the Ar--Ru interaction is represented by a pairwise sum of truncated Morse potentials.³¹ The ruthenium slab was thermalized together with the adsorbed nitrogen molecule until the surface temperature ($T_s=90\pm 5$ K) was maintained. The initial conditions for a trajectory, positions and velocities of the slab (including fictitious particles) and adsorbates atoms, were those obtained at the end of the thermalization procedure. To save computer time these initial conditions $\{R_i, V_i\}_0$ were stored and used to construct the initial conditions for the next $N_{\text{start}}=9$ trajectories. This procedure was achieved by integrating the equations of motion for the slab, fictitious and adsorbate particles for additional 500 time steps starting with $\{R_i, V_i\}_0$. For each of the N_{start} trajectories a different seed for the random number generator was used. It was verified that the results of the simulation were independent of the value of N_{start} in the range $15 \geq N_{\text{start}} \geq 0$. For each set of initial collider energy and incidence angle, 1000–5000 trajectories were calculated. The maximum integration time was taken to be 10 ps.

The results of the MD simulations showing the calculated cross section for CID as a function of the incident Ar or Kr atom kinetic energy are presented in Fig. 2 as filled symbols together with the experimental data points (open symbols).

The cross section has been calculated as an integral of the opacity function $P(b)$ over the relevant impact parameter (b) range [Eq. (6)]²³

$$\sigma_{\text{des}}=2\pi \int_0^{b_{\text{max}}} b \cdot P(b) \cdot db. \quad (6)$$

We found that the calculated threshold energy is 0.5 ± 0.1 eV, similar to the HSHC model predictions. This calculated number is obtained with the binding energy of nitrogen to the surface set at 0.25 eV. This value is derived from best fit of TPD line shapes analysis for the desorption of N_2 from $\text{Ru}(001)$ with a preexponential factor of 10^{12} s^{-1} . It is interesting to note that a much higher binding energy value of 0.44 eV has been often used in the literature.^{22,23} Using the higher binding energy number in our calculations, we could

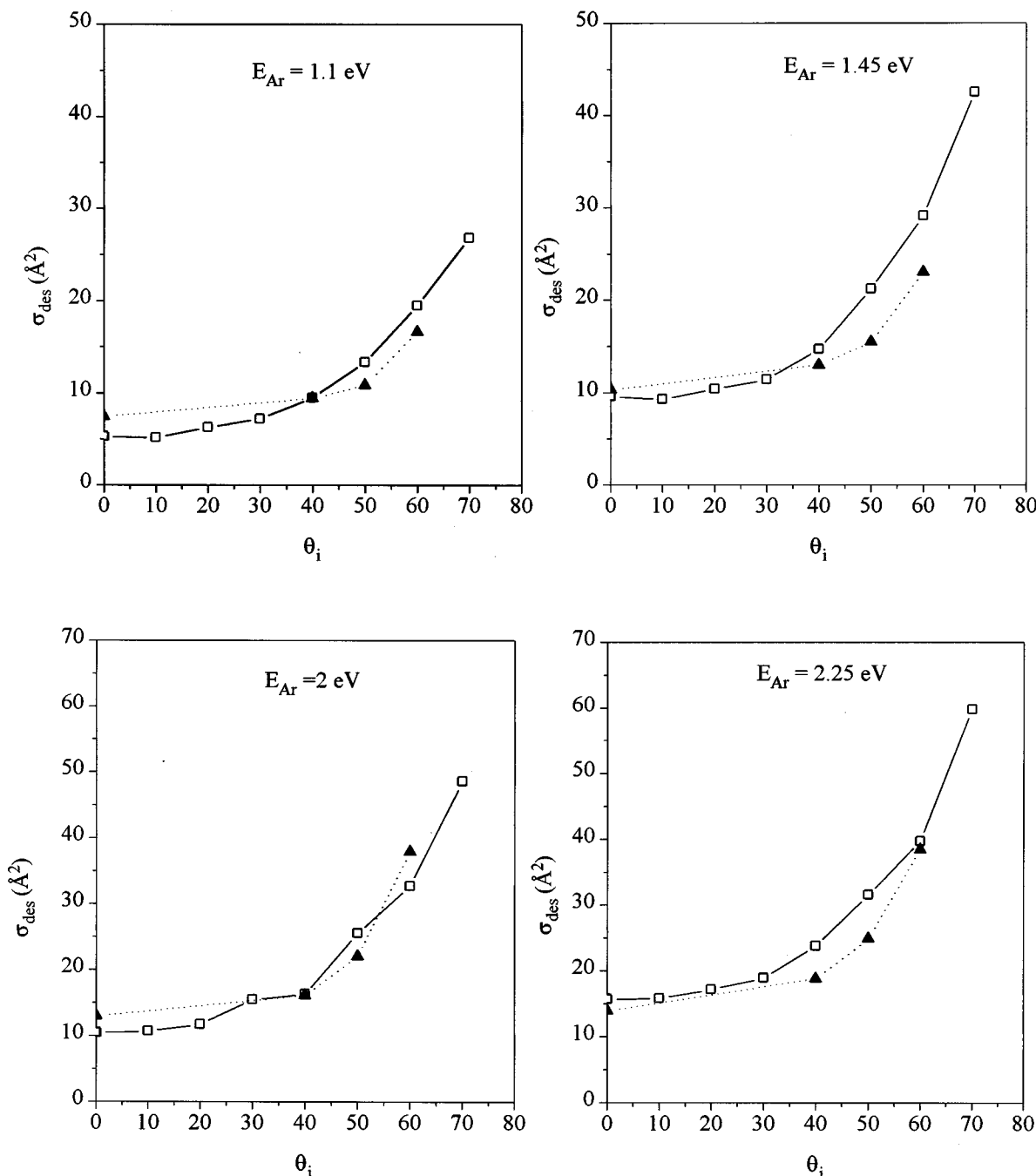


FIG. 8. Comparison of the angular dependence between experimentally measured and calculated CID cross sections for four initial energies of Ar: 1.1 eV; 1.45 eV; 2 eV, and 2.25 eV. Experimental results are shown as open squares, results of calculation are shown as filled triangles.

not have obtained the level of agreement shown in Fig. 2. This indirect way of verifying and in some cases the only way to determine binding energy of adsorbates to surfaces has been discussed by Levis and co-workers.^{10–12} The results of the MD simulations follow rather accurately the experimental data up to kinetic energy of about 2.5 eV at normal angle of incidence. Above this energy the calculated cross sections increase with a slower rate than the experimental data.

The dependence of σ_{des} on θ_i as predicted by the MD simulations is shown in Fig. 8 together with the corresponding experimental data. The overall trend of the increase of

σ_{des} at larger angles of incidence is nicely reproduced for all the collider's kinetic energies. At incident angle of 60° with respect to the surface normal σ_{des} grows by a factor of 3–4 compared with the value at normal incidence for all kinetic energies, in very good agreement with the experimental observations.

From the results of the simulations we conclude that the CID mechanism of N_2 from Ru(001) is dominated by a direct impulsive collision between the rare gas and the adsorbate. It was found that the opacity function defined in Eq. (6) contributes at distances up to 3 \AA at normal incidence, increas-

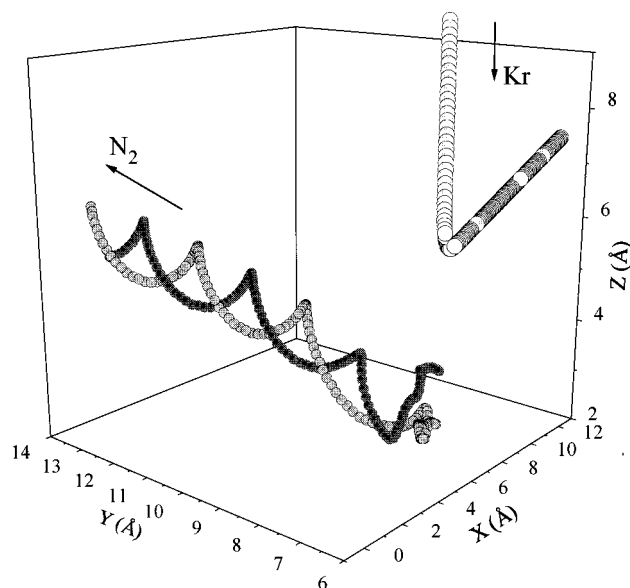


FIG. 9. A typical trajectory describing the collision between Kr and N_2 at $E_i=0.7$ eV and $\theta_i=0^\circ$. The impact parameter in this example is zero.

ing to about 7 Å at 60° angle of incidence and is only slightly incidence energy dependent. Coupling of the impulsive-tilt-motion of the nitrogen adsorbate with its motion normal to and away from the surface is observed in the majority of the trajectories. In some other trajectories, migration on the surface may also be coupled to desorption. A typical example of the behavior of such coupled motion is reproduced in Fig. 9. This new mechanism for CID is the reason for the enhanced CID yield at large angles of incidence, in which the collision induced tilt motion is particularly effective. Similar mechanism for CID has recently been reported in the case of oxygen on Ag(100), where corrugation in the tangential part of the molecule-surface potential was argued to be the reason for the enhanced CID at glancing angles.³⁰ Rotationally excited desorbed N_2 molecules are predicted to be formed as a result of impulsive-tilt-motion CID mechanism, as revealed in Fig. 9. The rotational excitation increases with incident energy of the collider, but decreases as the angle of incidence increases for the same energy. No vibrational excitation is predicted. Full account of this MD study will be presented in a subsequent work.²⁰

V. SUMMARY AND CONCLUSIONS

We have studied the dynamics of collision-induced desorption of N_2 molecules from Ru(001) surface by energetic rare gas atoms generated in a supersonic atomic beam source. Low initial coverage (0.01 ML of $^{15}N_2$) was chosen to model a CID process of an isolated molecule, thus, neglecting the effect of lateral N_2 - N_2 interactions. The cross sections for CID of nitrogen molecules, $\sigma_{des}(E_i, \theta_i)$, as a function of the kinetic energy and angle of incidence of Ar and Kr colliders have been determined at surface temperature of 96 K. It was found that $\sigma_{des}(E_i, \theta_i=0^\circ)$ changes monotonically in the range 0–25 Å², when the collider energy varies from threshold energy for desorption to the maximum energy of 5.5 eV. The cross section for desorption was in-

sensitive to the type of collider (Ar, Kr) or to the adsorbate isotope ($^{14}N_2$, $^{15}N_2$). The threshold energy for desorption equals 0.50 ± 0.10 eV, which is twice the binding energy of N_2 to Ru(001). The threshold energy for CID was found to be rather insensitive to the angle of incidence. This observation emphasizes the unique sensitivity of the CID of N_2 from Ru(001) to the parallel energy transferred during the collision.

The cross section for CID at a fixed collider's energy rises approximately four times as the incidence angle θ_i increases from 0° to 70°. The $\sigma_{des}(\theta_i)$ essentially scales with the tangential energy of the collider for angles above 30°.

Classical molecular dynamics simulations were performed to gain better understanding of the CID process. The experimental threshold energy and angular dependence of the cross section were reproduced very well by the simulations. The predominant mechanism for desorption was established to be a direct impulsive collision. A new collision induced, impulsive-tilt-motion mediated mechanism for desorption is shown to dominate the CID process of N_2 from Ru(001).

ACKNOWLEDGMENTS

This work has been partially supported by a grant from the Israel Science Foundation and by the German Israel Foundation. The Farkas Center for Light Induced Processes is supported by the Bundesministerium für Forschung und Technologie and the Minerva Gesellschaft für die Forschung mbH.

- ¹D. P. Woodruff and T. A. Delchar, *Modern Techniques of Surface Science*, 2nd ed. (Cambridge University Press, Cambridge, 1994).
- ²Y. Zeiri, J. J. Low, and A. Goddard, III, *J. Chem. Phys.* **84**, 2408 (1986).
- ³J. D. Beckerle, A. D. Johnson, and S. T. Ceyer, *Phys. Rev. Lett.* **62**, 685 (1989).
- ⁴S. T. Ceyer, *Annu. Rev. Phys. Chem.* **39**, 479 (1988).
- ⁵J. D. Beckerle, A. D. Johnson, and S. T. Ceyer, *J. Chem. Phys.* **93**, 4047 (1990).
- ⁶G. Ertl, in *Catalysis, Science, and Technology*, edited by J. R. Anderson and M. Boudart (Springer, Heidelberg, 1983), Vol. 4, p. 210.
- ⁷W. Tsai and W. H. Weinberg, *J. Phys. Chem.* **91**, 5302 (1987).
- ⁸R. M. Logan and R. E. Stickney, *J. Chem. Phys.* **44**, 195 (1966).
- ⁹R. M. Logan, in *Solid State Surface Sciences* (Marcel Dekker, New York, 1973), Vol. 3, p. 1.
- ¹⁰G. Szulczewski and R. J. Levis, *J. Chem. Phys.* **98**, 5974 (1993).
- ¹¹G. Szulczewski and R. J. Levis, *J. Chem. Phys.* **103**, 10238 (1995).
- ¹²D. Velic and R. J. Levis, *J. Chem. Phys.* **104**, 9629 (1996).
- ¹³Y. Zeiri, *Surf. Sci.* **231**, 408 (1990).
- ¹⁴Y. Zeiri and R. R. Lucchese, *J. Appl. Phys.* **94**, 4055 (1991).
- ¹⁵Y. Zeiri and R. R. Lucchese, *Surf. Sci.* **264**, 197 (1992).
- ¹⁶B. Kulginov, M. Persson, and C. T. Rettner, *J. Chem. Phys.* **106**, 3370 (1997).
- ¹⁷A. B. Anton, N. R. Avery, T. E. Madey, and W. H. Weinberg, *J. Chem. Phys.* **85**, 507 (1986).
- ¹⁸R. A. de Paola, F. M. Hoffmann, D. Heskett, and E. W. Plummer, *Phys. Rev. B* **35**, 4236 (1987).
- ¹⁹H. Bludau, M. Gierer, H. Over, and G. Ertl, *Chem. Phys. Lett.* **219**, 452 (1994).
- ²⁰L. Romm, Y. Zeiri, and M. Asscher (unpublished).
- ²¹L. Romm, G. Katz, R. Kosloff, and M. Asscher, *J. Phys. Chem. B* **101**, 2213 (1997).
- ²²P. Feulner and D. Menzel, *Phys. Rev. B* **25**, 4295 (1982).
- ²³R. D. Levine and R. B. Bernstein, *Molecular Reaction Dynamics and Chemical Reactivity* (Oxford University Press, New York, 1987).

- ²⁴J. D. Beckerle, A. D. Johnson, Q. Y. Yang, and S. T. Ceyer, *J. Chem. Phys.* **91**, 5756 (1989).
- ²⁵H. E. Pfnür, C. T. Rettner, J. Lee, R. J. Madix, and D. J. Auerbach, *J. Chem. Phys.* **85**, 7452 (1986).
- ²⁶A. González Ureña, *J. Phys. Chem.* **96**, 8212 (1992).
- ²⁷D. Velic and R. J. Levis, *Chem. Phys. Lett.* **269**, 59 (1997).
- ²⁸E. S. Hood, B. H. Toby, and W. H. Weinberg, *Phys. Rev. Lett.* **55**, 2437 (1985).
- ²⁹A. B. Anton, N. R. Avery, B. H. Toby, and W. H. Weinberg, *J. Electron Spectrosc. Relat. Phenom.* **29**, 181 (1983).
- ³⁰L. Vattuone, P. Gambardella, F. Cemic, U. Valbusa, and M. Rocca, *Chem. Phys. Lett.* **278**, 245 (1997).
- ³¹M. Head-Gordon and J. C. Tully, *J. Chem. Phys.* **95**, 9266 (1991); *Surf. Sci.* **268**, 113 (1992).
- ³²N. E. Henriksen, G. D. Billing, and Y. Hansen, *Surf. Sci.* **227**, 224 (1990).
- ³³H. Shi, K. Jacobi, and G. Ertl, *J. Chem. Phys.* **102**, 1432 (1995).